Eur. Phys. J. B **27**, 55–62 (2002)
DOI: 10.1140/epjb/e20020129

THE EUROPEAN PHYSICAL JOURNAL B
EDP Sciences

A phenomenological theory of giant magnetoelastic response in martensite

V.A. L'vov[1,a], S.P. Zagorodnyuk[1], and V.A. Chernenko[2]

[1] Department of Radiophysics, Taras Shevchenko University, Glushkov str. 2, 03022 Kiev-22, Ukraine
[2] Institute for Magnetism, Ukrainian Academy of Sciences, Vernadskii str. 36, 03142 Kiev-142, Ukraine

Received 18 November 2001 and Received in final form 26 January 2002

Abstract. The interrelation between the giant magnetoelastic response and the superelastic or/and rubber-like behavior of a martensitic alloy is substantiated. The equivalence principle for the mechanical and magnetoelastic stresses is formulated and then used for the quantitative theoretical description of the field-induced deformation of martensite. Two different orientations of the magnetic field with respect to the crystal axes are considered. The agreement between the theoretical and experimental field dependencies of the deformation is achieved.

PACS. 81.30.Kf Martensitic transformations – 75.80.+q Magnetomechanical and magnetoelectric effects, magnetostriction – 75.30.Gw Magnetic anisotropy

1 Introduction

A sufficiently large number of metallic alloys undergoes a martensitic phase transformation on cooling below a certain temperature T_{ms} referred to as the martensite start temperature (see [1–3]). Martensitic transformation (MT) is characterized by the spontaneous deformation of the cubic crystal lattice. For the cubic-tetragonal, cubic-orthorhombic and cubic-rhombohedral MT-s the strains $\hat{\varepsilon}_M$ occurring in the temperature range $T < T_{ms}$ typically are about few percents. The low-temperature phase is a spatially inhomogeneous state (martensite) formed by different variants (crystallographic domains) of this phase. The microstructure of martensite in many cases is very sensitive to mechanical stressing. The martensitic structure variation under the action of mechanical stresses gives rise to the physical phenomena, which are interesting for both fundamental studies and applications. Among these phenomena the superelasticity, rubber-like behavior and shape-memory effect are now of common knowledge [4].

Some martensitic alloys are ferromagnetic. Their Curie temperatures T_C may be both higher or lower than martensite start temperature [5–8]. The Ni–Mn–Ga [9,10], Fe–Pd [11] and Fe–Pt [12] ferromagnetic alloys are of special interest because the substantial change in the martensitic structure of these alloys can be induced not only by the mechanical stressing but also by the magnetic field application. As far as the change in the alloy morphology is accompanied by deformation, the giant magnetoelastic response of the ferromagnetic martensite is observed [9–11]. Very recently the field-induced strains about 5% have been reported for Ni–Mn–Ga alloy (see, for example [13]).

Different approaches to the theoretical description of the ferromagnetic martensite have been elaborated. Some of the proposed theoretical models [10,11,14] consider the volume fractions of martensite variants as the thermodynamical variables in the spirit of the local equilibrium concept (see, for example, [15,16]). These models are focused on the thermodynamical analysis of the magnetic-field-induced deformations of martensite without consideration of the physical interactions causing these deformations.

Another approach to the theoretical study of ferromagnetic martensite is close to the traditional Landau theory and is referred to as the phenomenological magnetoelastic model [17–22]. A spin-lattice interaction is explicitly regarded in this model by the introduction of the appropriate terms into the Landau potential. In this way, the magnetic anomalies accompanying MT have been described [17,19], and the phase diagram of ferromagnetic martensite has been constructed [18]. Furthermore, the resemblance between the ordinary mechanical stressing of the specimen and the stressing caused by the magnetic field application has been used for the evaluation of magnetoelastic response in martensite [19–21]. At the same time, the dependencies of the field-induced strains on the magnetic field value $\hat{\varepsilon}(H)$ have not been analyzed in the framework of thermoelastic model.

In this paper the possibility of quantitative description of $\hat{\varepsilon}(H)$ dependencies in the framework of magnetoelastic model is substantiated. The difference in the experimental curves obtained in [9] for the different field directions is

[a] e-mail: victorlvov@svitonline.com

explained. The quantitative agreement between the theoretical and experimental curves $\hat{\varepsilon}(H)$ is achieved for the specimens of the almost stoichiometric Ni_2MnGa alloy studied very recently in [22].

2 The equivalence principle for the magnetoelastic and mechanical stresses

According to magnetoelastic model [17–20] the Gibbs potential of the biaxially stressed cubic crystal is

$$G = F_e + F_m + F_{me} - \frac{1}{6}\left(\sigma_2 u_2 + \sigma_3 u_3\right), \qquad (1)$$

where

$$u_2 = \sqrt{3}\left(\varepsilon_{xx} - \varepsilon_{yy}\right),\ u_3 = 2\varepsilon_{zz} - \varepsilon_{yy} - \varepsilon_{xx},$$
$$\sigma_2 = \sqrt{3}\left(\sigma_{xx} - \sigma_{yy}\right),\ \sigma_3 = 2\sigma_{zz} - \sigma_{yy} - \sigma_{xx},$$

ε_{ii} and σ_{ii} are the strain and stress tensors components, coordinate axes x, y and z are oriented along [100], [010] and [001] crystallographic directions respectively.

The first term of the sum (1) describes the Helmholtz free energy of the elastic strains and can be presented in the form

$$F_e = \frac{3}{2}(C_{11} + 2C_{12})u_1^2 + \frac{1}{6}C'\left(u_2^2 + u_3^2\right), \qquad (2)$$

where C_{11}, C_{12} and $C' = (C_{11} - C_{12})/2$ are the elastic moduli of cubic crystal, $u_1 = (\varepsilon_{xx} + \varepsilon_{yy} + \varepsilon_{zz})/3$. Equation (2) expresses the ordinary elastic energy of cubic crystal in terms of $u_1 - u_3$ variables (see [23]).

The second term in (1) is the free energy of magnetic subsystem of the crystal. This energy can be expressed as

$$F_m = \frac{1}{2}J(T)\,y^2(T) + \frac{1}{2}M^2(T)\left(\mathbf{m}\cdot\mathbf{D}\cdot\mathbf{m}\right) - \mathbf{mH}M(T), \qquad (3)$$

where the first term is the spin exchange energy, the second term is the magnetostatic energy caused by the magnetic dipole-dipole interaction and the third term is the energy of magnetization vector $\mathbf{M}$ in the magnetic field $\mathbf{H}$. The roles of the exchange and magnetostatic energies in the properties of ferromagnetic martensites is analyzed in [22,11], respectively. All the energies are expressed in terms of the dimensionless variables $\mathbf{m} = \mathbf{M}(T)/M(T)$ and $y(T) = M(T)/M(0)$. The terms of the forth and sixth order in these variables are comparatively small [17] and therefore disregarded.

The third summand in (1) describes the interrelation between the magnetization and strains. This interrelation is caused by the spin-lattice interaction existing in all solids which include the paramagnetic ions. The energy of magnetoelastic coupling is conventionally described by the expression [17,18,22]:

$$F_{me} = -\delta_0 y^2(T)u_1 - \delta_1\Big[\sqrt{3}\left(m_x^2 - m_y^2\right)u_2 + \left(2m_z^2 - m_y^2 - m_x^2\right)u_3\Big], \qquad (4)$$

where δ_0 and δ_1 are the magnetoelastic parameters. The parameter δ_0 is responsible for volume magnetostriction and δ_1 causes the magnetostrictive shear deformation of the crystal lattice.

The role of magnetoelastic coupling in the properties of martensitic alloys becomes clear when the formula (1) is rewritten in the following form:

$$G = F_e + F_m - \delta_0 y^2(T)u_1 - \frac{1}{6}\left(\sigma_2^{\mathit{eff}}u_2 + \sigma_3^{\mathit{eff}}u_3\right), \qquad (5)$$

where

$$\sigma_2^{\mathit{eff}} = \sigma_2 + \sigma_2^{me},\quad \sigma_3^{\mathit{eff}} = \sigma_3 + \sigma_3^{me},$$
$$\sigma_2^{me} = 6\sqrt{3}\delta_1\left(m_x^2 - m_y^2\right),$$
$$\sigma_3^{me} = 6\delta_1\left(2m_z^2 - m_y^2 - m_x^2\right). \qquad (6)$$

The functions σ_2^{eff} and σ_3^{eff} can be interpreted as the "effective stresses" [19,20]. These stresses are the sums of the mechanical stresses σ_2, σ_3 and magnetoelastic ones $\sigma_2^{me}, \sigma_3^{me}$. The former are related to the external forces applied to the specimen, the latter depend on the direction of the unit magnetic vector $\mathbf{m}$ and therefore, a rotation of the magnetic vector under the action of the magnetic field results in the additional stressing of the alloy. The field-induced stresses are

$$\sigma_{2,3}(H) = \sigma_{2,3}^{me}(H) - \sigma_{2,3}^{me}(0). \qquad (7)$$

For the parent phase the field-induced strains can be explicitly expressed through the stresses (7). The conditions $\partial(F_e + F_{me})/\partial u_{2,3} = 0$ result in the ordinary stress–strain relationships of the linear elasticity theory

$$u_{2,3}(H) = \sigma_{2,3}(H)/2C', \qquad (8)$$

(for more detail see [17]). Similarity between the mechanical and field-induced stresses follows immediately from the expressions (5) and (6): Gibbs potential involves mechanical and magnetoelastic stress tensors in combination $\hat{\sigma}^{\mathit{eff}} = \hat{\sigma} + \hat{\sigma}^{me}(0) + \hat{\sigma}(H)$, and therefore, the results of its minimization will be the same for $\hat{\sigma}^{\mathit{eff}} = \hat{\sigma}^{me}(0) + \hat{\sigma}(H)$ and $\hat{\sigma}^{\mathit{eff}} = \hat{\sigma}^{me}(0) + \hat{\sigma}$. (The caret on the letter symbolize the totality of tensor components). Thus, the field-induced deformation is equal to the deformation caused by the mechanical load if the field-induced stress tensor $\hat{\sigma}(H)$ is equal to the stress tensor $\hat{\sigma}$ induced by the loading of the experimental specimen. This conclusion may be referred to as the *equivalence principle* for the mechanical and magnetoelastic deformation.

A martensitic structure rearrangement accompanying mechanical stressing of the shape-memory alloys causes a superelasticity and rubber-like behavior of these alloys.

It means, that the stiffness coefficient relating the applied mechanical stress to the resultant deformation of the alloy is substantially smaller, than C' modulus measured in the parent phase well above the MT temperature range. Thus, for the initial part of the $\sigma - \varepsilon$ curve

$$\varepsilon(\sigma) \approx (\partial\varepsilon/\partial\sigma)_0 \, \sigma, \tag{9}$$

where $(\partial\varepsilon/\partial\sigma)_0 \gg 1/C'$.

A magnetoelastic response of the spatially inhomogeneous martensitic phase cannot be evaluated from the formula (8) because the magnetic field application results not only in the elastic deformation of the crystal lattice but in the variation of martensite microstructure as well [9–11,24,25]. In accordance with the equivalence principle we can assert that the expression for the field-induced deformation of martensite is similar to (9), *i.e.*

$$\hat{\varepsilon}(H) \approx (\partial\hat{\varepsilon}/\partial\sigma_\beta) \cdot \sigma_\beta(H), \tag{10}$$

where the coefficients $(\partial\hat{\varepsilon}/\partial\sigma_\beta)$ are of the order of experimental value $(\partial\varepsilon/\partial\sigma)_0$ obtained from the ordinary mechanical tests of the alloy, $\beta = 2, 3$. It can be concluded therefore, that the giant magnetoelastic response of the ferromagnetic martensite is essentially a superelastic or/and rubber-like behavior of the alloy caused by the field-induced stresses. This conclusion explains a substantial spread in the experimental values of magnetoelastic response reported by the different authors for the different alloys of Ni–Mn–Ga alloy system: the initial slopes and the general forms of the $\sigma - \varepsilon$ curves describing the superelastic behavior of these alloys strongly depend on their temperature, composition and preliminary treatment.

3 Field-induced deformations

The field dependence of magnetoelastic stresses can be found immediately from the phenomenological theory of ferromagnetic martensite, developed in [17] if the field-induced deformations (10) are substantially smaller than the spontaneous strains accompanying a cubic-tetragonal martensitic transformation of the alloy. According to this theory, a simple interrelation exists between the magnetic anisotropy energy of the martensitic phase, magnetoelastic constant δ_1 and parameter $u_0 = 2(c_t - a_t)/a_t$ characterizing spontaneous strains (a_t and c_t are the parameters of tetragonal unit cell).

Tetragonal lattice with the principal symmetry axis directed closely to [100], [010], or [001] direction of parent phase may be referred to as the x-, y- or z-variant of tetragonal phase correspondingly. For the periodic kj-microstructure formed by the alternating k- and j-variants (Fig. 1) the average spontaneous strains can be approximated as

$$\begin{aligned} \bar{\varepsilon}_{ii} &= -u_0/6, \quad \bar{\varepsilon}_{jj} = (2 - 3\alpha)\, u_0/6, \\ \bar{\varepsilon}_{kk} &= (3\alpha - 1)\, u_0/6, \end{aligned} \tag{11}$$

where α and $1 - \alpha$ are the fractions of tetragonal variants, $k \neq i \neq j$.

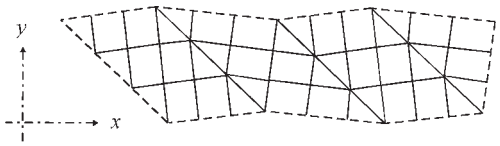

Fig. 1. The idealized martensitic structure formed by the alternating x- and y-domains of the tetragonal crystal lattice.

The microstructure elements being typical for the large number of martensites are better visible in the electron microscope. By contrast, the ferromagnetic domains are usually observed in the scales available for the optical microscopy. In the case when the period of the martensite microstructure is substantially smaller than the dimensions of ferromagnetic domains, the magnetic vectors $\mathbf{m}$ of the domains are coupled with the average strains (11) rather than with the strains inherent to the individual martensite variants. The substitution of the averaged functions $u_2^M = \sqrt{3}\,(\bar{\varepsilon}_{xx} - \bar{\varepsilon}_{yy})$, $u_3^M = 2\bar{\varepsilon}_{zz} - \bar{\varepsilon}_{yy} - \bar{\varepsilon}_{xx}$ in the formula (4) results in the expression

$$\begin{aligned} F_m + F_{me} = \frac{1}{2} J^*(T)\, y^2(T) + A_1 m_i^2 + A_2 m_j^2 \\ + \frac{1}{2} M^2(T)\, (\mathbf{m} \cdot \mathbf{D} \cdot \mathbf{m}) - \mathbf{m}\mathbf{H} M(T), \end{aligned} \tag{12}$$

where $J^*(T) = J(T) - 2\delta_0 u_1$ is the exchange integral renormalized by the volume magnetostriction, $A_1 = 3\delta_1 u_0 \alpha$ and $A_2 = 3\delta_1 u_0 (2\alpha - 1)$ are the magnetic anisotropy parameters. Magnetic properties of the microtwinned ferromagnetic martensite characterized by two anisotropy constants were considered in [17,19]. A good agreement between the theoretical results and experimental data obtained in [5,7] was achieved.

Meanwhile, the interaction between the very small magnetic domains and comparatively large elastic twins of tetragonal phase was observed very recently in Ni–Mn–Ga specimens exhibiting a giant magnetoelastic response [24,25]. As far as the period of twinning exceeds in this case the dimensions of the magnetic domains, the magnetoelastic interaction between the magnetic vector and the tetragonal martensite variants takes place. The relevant expression for the energy $F \equiv F_m + F_{me}$ can be obtained immediately from the expression (12): the case $\alpha = 0$ corresponds to the j-variant of the tetragonal phase and the expression with $\alpha = 1$ describes the energy of k-variant. Moreover, it is worth to express the energy through the angular variables φ, ψ related to the Descartes coordinates of magnetic vector as

$$m_x = \sin\psi \cos\varphi, \quad m_y = \sin\psi \sin\varphi, \quad m_z = \cos\psi$$

and to analyze the case of the "easy axis" type of magnetic anisotropy ($\delta_1 u_0 > 0$) actual, for example, for Ni–Mn–Ga alloys with martensite start temperature $T_{ms} < T_C$. Further consideration will be carried out for the ellipsoidal specimen and the axes of ellipsoid will be aligned with $[\bar{1}10]$, $[1\bar{1}0]$ and [001] directions. In these axes a demagnetization matrix is diagonal, its elements will be denoted as D_1, D_2, D_3, respectively.

3.1 Deformations induced by the field H‖[001]‖z

For x-variant of tetragonal phase $\alpha = 0$, $j = x$ and therefore

$$F = M^2(T)\left[\frac{1}{2}D'\cos^2\psi - (a\cos^2\varphi - D_{xy}\sin\varphi\cos\varphi)\sin^2\psi\right] - HM(T)\cos\psi, \quad (13)$$

where

$$a = 3\delta u_0, \quad \delta = \delta_1/M^2(T),$$
$$D_{xy} = (D_1 - D_2)/2,$$
$$D' = D_3 - (D_1 + D_2)/2.$$

A dimensionless constant a describes the magnetic anisotropy of tetragonal crystal lattice, δ is a dimensionless magnetoelastic constant, D_{xy} and D' are the elements of demagnetization matrix in the coordinate system associated with the axes *1*, *2*, *z* of ellipsoidal specimen (see Fig. 2). The extremum conditions $\partial F/\partial\varphi = 0$ and $\partial F/\partial\psi = 0$ result in the equations

$$\cos\psi \equiv \cos\psi_{[001]} = \begin{cases} H/H_{S1}, & H < H_{S1}, \\ 1, & H \geq H_{S1}, \end{cases} \quad (14)$$

where

$$H_{S1} = M(T)\left[D' + 2(a\cos^2\varphi_1 - D_{xy}\sin\varphi_1\cos\varphi_1)\right], \quad (15)$$

and

$$\cos^2\varphi_1 = \frac{1}{2} + \frac{a}{2\sqrt{a^2 + D_{xy}^2}},$$
$$\sin\varphi_1\cos\varphi_1 = -\frac{D_{xy}}{2\sqrt{a^2 + D_{xy}^2}}\cdot$$

Equations (14) describe vector **m** rotation in the fixed plane $\varphi = \varphi_1$. The field value $H = H_{S1}$ corresponds to the magnetic saturation of x-variant. The magnetic vector of the y-variant of tetragonal phase rotates in the plane $\varphi_2 = \pi/2 - \varphi_1$ and the saturation field is equal to H_{S1}. The magnetic vector of the z-variant is aligned with applied magnetic field.

The averaged field-induced stresses can be found for the case when the volume fractions of x- y- and z-variants are equal to each other. In this case

$$\langle\sigma_2(H)\rangle = 6\sqrt{3}\delta M^2(T)\sin^2\psi_{[001]} \times \frac{1}{3}\left(\cos 2\varphi_1 + \cos 2\varphi_2\right), \quad (16)$$
$$\langle\sigma_3(H)\rangle = \frac{2}{3}18\delta M^2(T)\cos^2\psi_{[001]}.$$

As far as $\cos 2\varphi_1 = -\cos 2\varphi_2$, the $\sigma_2(H)$ stress components induced in x- and y-variants have the same absolute value but differs in sign and therefore, compensate each other in average. Moreover, for z-variant of martensite the field induced stresses are absent in view of the steady vector **m** direction. Thus, the experimentally measured giant magnetoelastic response is caused by the stress component $\sigma_3(H)$ and the formula for the macroscopic deformation is

$$\langle\hat{\varepsilon}(H,T)\rangle \approx \frac{2}{3}\left(\partial\hat{\varepsilon}/\partial\sigma_3\right)18\delta M^2(T)\cos^2\psi_{[001]}. \quad (17)$$

Factor 2/3 occurs in the expression (17) because x-, y- and z-variants of the martensite are, generally speaking, equiprobable and only two of them contribute to the field-induced deformation. Expression (17) predicts strong temperature dependence of the field-induced deformation of martensite in the temperature ranges close to T_{ms}, T_C or intermartensitic transformations temperatures, because $\partial\hat{\varepsilon}/\partial\sigma_3$ and/or M values critically depend on the temperature in these ranges. A possibility of the giant magnetoelastic response in the two-phase state existing in the vicinity of martensite start temperature was deduced theoretically in [20] and confirmed experimentally in [26].

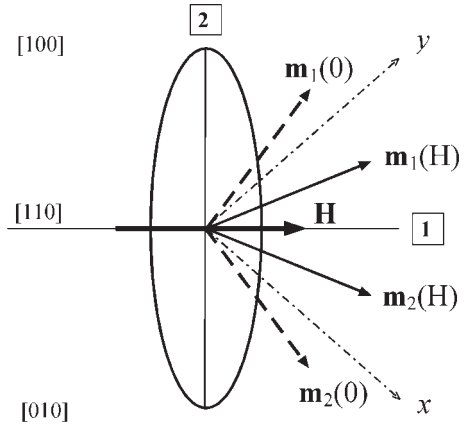

Fig. 2. Magnetic vectors rotation in x- and y-variants of tetragonal phase. A magnetic field is applied to the ellipsoidal specimen in [110] direction. The numbers in the squires mark the ellipsoid axes correspondent to the demagnetization factors D_1 and D_2.

3.2 Deformations induced by the field H‖[110]

When the magnetic field is oriented in [110] direction the sum of the magnetic and magnetoelastic energies of x-variant can be expressed as

$$F = M^2(T)\left[\frac{1}{2}D'\cos^2\psi - (a\cos\varphi - D_{xy}\sin\varphi)\cos\varphi\sin^2\psi\right] - \left[HM(T)/\sqrt{2}\right](\cos\varphi + \sin\varphi)\sin\psi. \quad (18)$$

The relevant expression for y-variant can be obtained from (18) by the transposition $\cos\varphi \rightleftarrows \sin\varphi$. For z-variant of

tetragonal phase the formula

$$F = M^2(T)\Big[\frac{1}{2}(D' - 2a)\cos^2\psi + D_{xy}\sin\varphi\cos\varphi\sin^2\psi\Big] - \Big[HM(T)/\sqrt{2}\Big](\cos\varphi + \sin\varphi)\sin\psi \quad (19)$$

is valid.

The conditions $\partial F/\partial\varphi = 0$ and $\partial F/\partial\psi = 0$ result in the following conclusions.

Magnetic field rotates the magnetic vectors $\mathbf{m}_1$ and $\mathbf{m}_2$ of x- and y-variants in such a way that

$$m_{1z} = m_{2z} = 0, \quad m_{1x}^2 = m_{2y}^2, \quad m_{1y}^2 = m_{2x}^2$$

for the any value of the magnetic field (Fig. 2). In this case the field-induced stress component $\sigma_3(H)$ is equal to zero for both of variants, while the $\sigma_2(H)$ component inherent in the x-variant differs in sign from one applied to y-variant, and therefore, these components compensate each other. Thus, the x- and y-variants do not contribute to the macroscopic deformation.

The field rotates a magnetic vector $\mathbf{m}_3$ of z-variant in the fixed plane $\varphi = \pi/4$. For the specimen with $D_2 = D_3$ the equations for the rotation angle ψ are

$$\sin\psi \equiv \sin\psi_{[110]} = \begin{cases} H/H_{S2}, & H < H_{S2}, \\ 1, & H \geq H_{S2}, \end{cases} \quad (20)$$

where the magnetic saturation field H_{S2} is related to the magnetic anisotropy parameter a and demagnetization coefficients D_1, D_3 as $H_{S2} = M(T)(2a + D_1 - D_3)$. As far as $m_{3x} = m_{3y} = \text{const.}$, the component $\sigma_2(H)$ is equal to zero. At the same time, the magnetic field induces a nonzero stress component

$$\langle\sigma_3(H)\rangle = -\frac{1}{3}18\delta M^2(T)\sin^2\psi_{[110]}. \quad (21)$$

Thus, the macroscopic deformation induced by the field oriented in [110] crystallographic direction is

$$\langle\hat{\varepsilon}(H,T)\rangle \approx -\frac{1}{3}(\partial\hat{\varepsilon}/\partial\sigma_3)\,18\delta M^2(T)\sin^2\psi_{[110]}. \quad (22)$$

The factor 1/3 occurs in the formula (22) because only one of the martensite variants induces the macroscopic deformation.

A comparison of the formulas (17) and (22) shows, that the deformation tensor components induced by the saturation field $H = H_{S2}$ applied in [110] direction differ by the factor $-1/2$ from the appropriate components induced by the field $H = H_{S1}$ applied along [001]. The difference in the saturation fields values is caused by the magnetostatic energy and therefore depends on the shape of the experimental specimen.

4 Computations

Following the works [22,27], we carry out the computation of magnetization and field-induced deformations with regard to the imperfectness of the crystal lattice. According to [22] the imperfectness of crystal structure results in the random dispersion s of u_1 variable. The "statistical" value of this variable is $u_1^{(s)} = u_1^{(0)} + s$, where $u_1^{(0)}$ characterizes the volume change accompanying cubic-tetragonal phase transformation. The renormalized exchange parameter J^* introduced in (12) depends on $u^{(s)}$, and hence, Curie temperature found from the equation $J^*(T,s) = 0$ is also randomly dispersed:

$$T_C^{(s)} = T_C + 2sT_C\delta_0/\zeta, \quad (23)$$

where ζ is the factor involved in the relationship $J^*(T,0) = \zeta(T - T_C)/T_C$ postulated in the Landau theory.

Physically $T_C^{(s)}$ values are the temperatures of the ferromagnetic ordering in the small spatial domains of the imperfect experimental specimen. For these domains the magnetization value $M(T,s) = M(0)y(T,s)$ may be found from the well-known equation of the magnetism theory

$$y(T,s) = \tanh\Big\{T_C^{(s)}y(T,s)/T\Big\}. \quad (24)$$

When the volume fractions of x- y- and z- variants are equal to each other the averaged magnetization of martensitic phase in the field applied in [001] direction is expressed as

$$\Big\langle M^{(s)}(H,T)\Big\rangle = M(T,s)\Big[\frac{1}{3}\Delta^{(s)}(H,T) + \frac{2}{3}\cos\psi_{[001]}^{(s)}(H,T)\Big], \quad (25)$$

where the function $\Delta^{(s)}(H,T) = (H/D_3M)$ for $H < D_3M$ and $\Delta^{(s)}(H,T) = 1$ for $H \geq D_3M$ ($M = M(T,s)$). The $\Delta^{(s)}$ function describes the magnetization process in z-variant of tetragonal lattice. This process is caused by the displacements of the domain walls separating magnetic domains with antiparallel magnetic vectors, and hence, is not associated with the field-induced deformation of the specimen. Magnetization of cubic phase may be by evaluated from the equation

$$\Big\langle M^{(s)}(H,T)\Big\rangle = M(T,s)\Delta^{(s)}(H,T). \quad (26)$$

The averaged magnetization is described by the formula

$$\Big\langle\overline{M(H,T)}\Big\rangle = \int_{-\infty}^{+\infty}\Big\langle M^{(s)}\Big\rangle f(s)\theta(T_C^{(s)} - T)\mathrm{d}s, \quad (27)$$

where

$$f(s) = \frac{1}{s_0\sqrt{2\pi}}\exp\left(-\frac{s^2}{2s_0^2}\right),$$

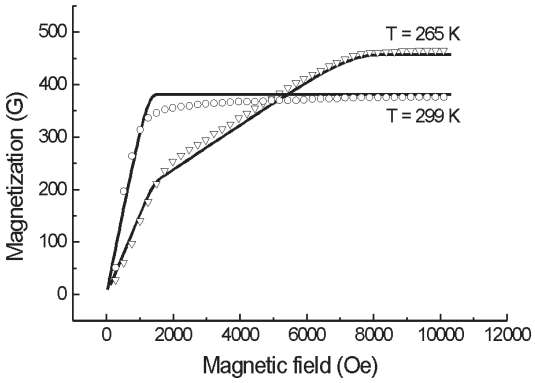

Fig. 3. Theoretical magnetization curves for the martensitic ($T = 265$ K) and austenitic ($T = 299$ K) phases of Ni–Mn–Ga alloy in the field parallel to [001] direction. Experimental dependencies obtained in [9] for the same temperatures and field direction are shown for comparison.

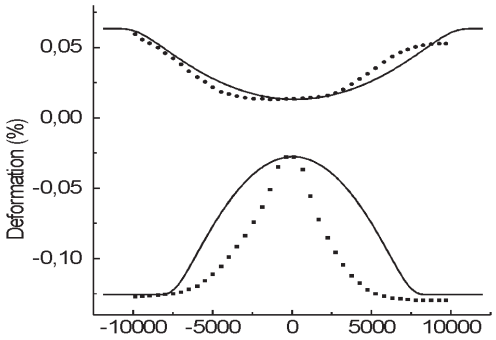

Fig. 4. Field-induced deformation ε_{001} computed for two directions of the magnetic field. Upper curve corresponds to the field applied in [110] direction and the lower one is plotted for the field aligned with [001]. The experimental points obtained in [9] are presented for comparison.

is Gauss distribution, $\theta(T_C^{(s)} - T)$ is a step-wise Heaviside function.

Now it should be noted that the expressions (17) and (22) for the field-induced deformation also depend on the random value s by means of the values M, $\psi_{[001]}$ and $\psi_{[110]}$. In such a case the average field-induced deformation should be computed from the formula

$$\left\langle \overline{\hat{\varepsilon}(H,T)} \right\rangle = 12\delta \left(\partial\hat{\varepsilon}/\partial\sigma_3\right) \times \left[\int_{-\infty}^{+\infty} M(T,s) \cos\psi_{[001]}^{(s)} f(s) \theta(T_C^{(s)} - T) \mathrm{d}s \right]^2, \quad (28)$$

when the magnetic field is aligned with [001], and

$$\left\langle \overline{\hat{\varepsilon}(H,T)} \right\rangle = -6\delta \left(\partial\hat{\varepsilon}/\partial\sigma_3\right) \times \left[\int_{-\infty}^{+\infty} M(T,s) \sin\psi_{[[110]}^{(s)} f(s) \theta(T_C^{(s)} - T) \mathrm{d}s \right]^2, \quad (29)$$

when the field is parallel to [110] direction.

Figure 3 shows a theoretical magnetization curve computed for the Ni–Mn–Ga specimen experimentally studied in [9]. We modelled this specimen, being a platelet oriented normally to [110] direction, by the ellipsoid flattened in this direction (see Fig. 2). In such a case $D_1 > D_2 = D_3$ and the D_1/D_2 ratio may be considered as a fitting parameter. All other parameters involved in the computations were taken from [9,17,19,22]. In particular, the value $\delta = -23$ was accepted for the dimensionless magnetoelastic constant. This value results from the estimation $\delta_1 = -1.2 \times 10^7$ erg/cm^3 obtained in [17,19] for the alloy with $M = 690$ G. Figure 3 illustrates a quantitative agreement between the theoretical results and experimental data reported in [9].

Figure 4 shows the field-induced deformation of the specimen in [001] direction computed for H applied in [001] and [110] directions. The $(\partial\varepsilon_{001}/\partial\sigma_3)$ value was used as the fitting parameter, without any changes in the parameters involved in the previous computations. A semi-quantitative agreement between the theoretical and experimental dependencies $\varepsilon_{001}(H)$ was achieved for the quite reasonable value $(\partial\varepsilon_{001}/\partial\sigma_3)^{-1} = 59$ MPa/percent: the experimental values $\mathrm{d}\sigma/\mathrm{d}\varepsilon \sim 100$ MPa/percent were obtained in the course of mechanical stressing of Ni–Mn–Ga alloys (see [28] and references therein). The strains shown in the Figure 4 are caused by both ordinary magnetostriction and comparatively small quasi-reversible rearrangement of martensite variants, because both processes correspond to the quasi-linear stress–strain dependence. The analysis of field-induced irreversible strains of about 5% experimentally observed in [13] requires an essential modification of the theory.

In order to prove that the absence of the rigorous quantitative agreement between the theoretical and experimental $\varepsilon_{001}(H_{001})$ dependencies is not of the fundamental significance, a theoretical analysis of the experimental data obtained in a very recent work [22] was carried out. The parallelepiped-shaped specimen with the dimensions $5 \times 7 \times 11.5$ mm^3 was modelled by the ellipsoid with the axes $A = B = 6$ mm, $C = 11.5$ mm. The values $T = 140$ K, $M(T) = 525$ G were taken for computations in accordance with real experimental conditions and previously accepted value $\delta = -23$ was used. Figure 5 illustrates a quantitative agreement between the theoretical and experimental $\varepsilon_{001}(H)$ curves achieved for $(\partial\varepsilon_{001}/\partial\sigma_3)^{-1} = 41$ MPa/percent.

5 Conclusions

The following conclusions about the physical nature of a giant magnetoelastic response in the martensites can be made on the basis of the equivalence principle formulated in this work for the mechanical and magnetoelastic stresses.

1. The giant magnetoelastic response observed in some martensitic alloys is a manifestation of the ordinary spin-lattice interactions (existing in all ferromagnetic solids) in

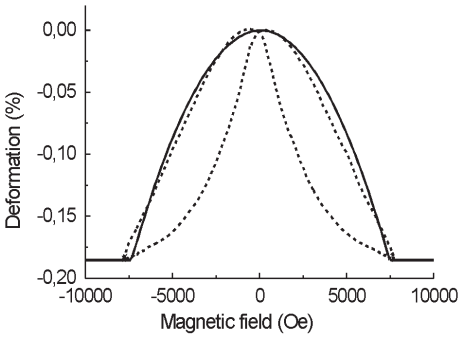

Fig. 5. Theoretical (solid line) and experimental (dashed line) curves describing the ε_{001} deformation induced by the magnetic field applied in [001] direction to the specimen studied in [22].

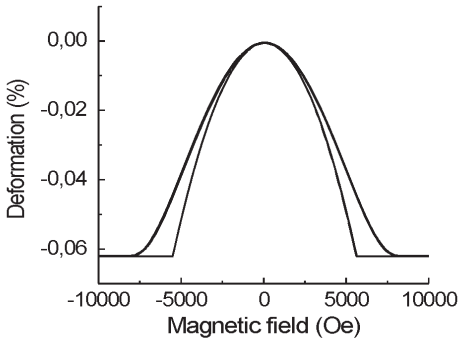

Fig. 6. The influence of the statistical dispersion of Curie temperature on the field dependence of deformation. The solid line computed for $s_0 = 0$, $(\partial\varepsilon_{001}/\partial\sigma_3)^{-1} = 59$ MPa/percent demonstrate parabolic dependence while the bold line obtained for $s_0 = 0.030$, $(\partial\varepsilon_{001}/\partial\sigma_3)^{-1} = 37$ MPa/percent exhibits the deviation from the parabola.

combination with the superelasticity or/and rubber-like behavior of these alloys.

2. A phenomenological magnetoelastic model of the ferromagnetic martensite developed in [17,19–21] enables a computation of the field-induced deformation of martensite. The model explains the difference in $\varepsilon_{001}(H_{001})$ and $\varepsilon_{001}(H_{110})$ dependencies observed in [9].

3. In the case of linear stress–strain dependence the computed field dependence of the deformation is close to quadratic; the experimental field dependence of the cycling deformation reported in the recent work [22] agrees well with the theoretical one at the reasonable value of stiffness coefficient relating the applied mechanical stress to the resultant deformation of the alloy (Fig. 5).

The deviations from the quadratic $\hat{\varepsilon}(H)$ dependence observed and intensively discussed in the literature may be caused by

i) the random spread in the local Curie temperatures, magnetization values and crystallographic directions inherent in the different spatial domains of the specimen (this statement is illustrated in Fig. 6);

ii) the hardly observable nonlinear character of the stress–strain dependencies for the very small values of the applied stresses $\sigma \sim 1$ MPa;

iii) the remaining parent phase inside the austenitic one;

iv) the nonequilibrium character of the martensitic phase;

v) the errors of experimental observation of the magnetoelastic response of the specimen being in contact with the data unit.

Factor i) was accounted above. The role of factors ii) – v) in the giant magnetoelastic response has not been analyzed till now, but ii), iii) can be considered in future in the framework of the phenomenological magnetoelastic model.

The equivalence principle for the mechanical and magnetoelastic stresses enables a preliminary estimation of the expected magnetoelastic response of the alloy from the stress–strain curves obtained before the performance of magnetostriction measurements.

It should be emphasized that the proposed theoretical approach for the description of giant magnetoelastic response in martensite is justified only in the case when the field-induced deformation of the alloy $\varepsilon(H,t)$ is substantially smaller than the spontaneous deformation ε_0 accompanying a complete martensitic transformation ($\varepsilon_0 \approx 5\%$ for the Ni–Mn–Ga alloys). If this condition is not observed, the magnetic field application results in the strong irreversible modification of the martensite microstructure and nonlinear stress–strain dependencies. In this case the expressions (10) cannot be used, and moreover, the irreversible character of the field-induced deformation process should be accounted.

V.A.C. is grateful to IEN Galileo Ferraris (Torino, Italy) and CNR, TeMPE (Lecco, Italy) for financing his stay at these Institutes. NATO Linkage Grant PST.CLG.977697 is gratefully acknowledged.

References

1. J.W. Christian, *The theory of transformations in metals and alloys* (Oxford, Pergamon Press, 1965).
2. C.M. Wayman, *Introduction to crystallography of martensitic transformations* (New York: MackMillan, 1964).
3. H. Warlimont, L. Delaey, *Martensitic transformations in copper- silver- and gold-based alloys* (Oxford: Pergamon Press, 1974).
4. K. Otsuka, X. Ren, Intermetallics **7**, 511 (1999).
5. P.J. Webster, K.R.A. Ziebeck, S.L. Town, M.S. Peak, Phil. Mag. B **49**, 295 (1984).
6. V.V. Kokorin, V.A. Chernenko, Phys. Met Metallogr. **65**, 190 (1989).
7. A.N. Vasil'ev, S.A. Klestov, R.Z. Levitin, V.V. Snegirev, V.V. Kokorin, V.A. Chernenko, JETP **82**, 524 (1996).
8. B. Zhang, T. Klemmer, D. Hoydick, W.A. Soffa, IEEE Trans. Mag. **30**, 589 (1994).
9. K. Ullakko, J.K. Huang, C. Kantner, R.C. O'Handley, V.V. Kokorin, Appl. Phys. Lett. **69**, 1966 (1996).
10. R.C. O'Handley, J. Appl. Phys. **83**, 3263 (1998).
11. R.D. James, M. Wuttig, Phil. Mag. A **77**, 1273 (1998).
12. T. Kakeshita, T. Takeuchi, T. Fukuda, M. Tsujiguchi, R. Oshima, S. Muto, Appl. Phys. Lett. **77**, 1502 (2000).

13. R.C. O'Handley, S.J. Murray, M. Marioni, H. Nembach, M.S. Allen, J. Appl. Phys. **87**, 4712 (2000).
14. A.A. Lichachev, K. Ullakko, Eur. Phys. J. B **14**, 263 (2000).
15. Y.I. Paskal, L.A. Monasevich, Sov. Phys. J. **78**, 1466 (1979).
16. C. Seguí, E. Cesari, J. Pons, Mat. Trans. JIM **33**, 650 (1992).
17. V.A. L'vov, E.V. Gomonaj, V.A. Chernenko, J. Phys. Cond. Matt. **10**, 4587 (1998).
18. A.N. Vasil'ev, A.D. Bozhko, V.V. Khovailo, *i.e.* Dikshtein, V.G. Shavrov, V.D. Buchel'nikov, M. Matsumoto, S. Suzuki, T. Takagi, J. Tani, Phys. Rev. B **59**, 1113 (1999).
19. V.A. Chernenko, V.A. L'vov, E. Cesari, JMMM **196–197**, 859 (1999).
20. V.A. Chernenko, V.A. Lvov, E. Cesari, P. McCormick, Mat. Trans. JIM **8**, 928 (2000).
21. V.A. Chernenko, O. Babii, V.A. Lvov, P.G. McCormick, Mat. Sci. Forum **327–328**, 485 (2000).
22. V.A. Chernenko, V.A. L'vov, M. Pasquale, S. Besseghini, C. Sasso, D.A. Polenur, Int. J. Appl. Electromagn. Mech. **12**, 3 (2000).
23. J.K. Liakos, G.A. Saunders, Phil. Mag. A **46**, 217 (1982).
24. R. James, R. Tickle, M. Wuttig, Mat. Sci. Eng. A **273–275**, 320 (1999).
25. H.D. Chopra, J. Chunhai, V.V. Kokorin, Phys. Rev. B **61**, 14913 (2000).
26. C.H. Yu, W.H. Wang, J.L. Chen, G.H. Wu, F.M. Yang N. Tang, S.R. Qi, W.S. Zhan, J. Appl. Phys. **87**, 6292 (2000).
27. V.P. Silin, D. Wagner, V.M. Zverev, Phys. Lett. A **199**, 395 (1995).
28. V.V. Martinov, V.V. Kokorin, J. Phys. III France **2**, 739 (1992).